PREDICTION OF WOOD QUALITY IN SMALL-DIAMETER DOUGLAS-FIR USING SITE AND STAND CHARACTERISTICS

C. D. Morrow
Graduate Student
E-mail: carl.morrow@vandals.uidaho.edu

*T. M. Gorman**†
Professor
Forest Products Program
University of Idaho
Moscow, ID 83844-1132
E-mail: tgorman@uidaho.edu

J. W. Evans
Mathematical Statistician
E-mail: jwevans@fs.fed.us

D. E. Kretschmann†
Research General Engineer
E-mail: dkretschmann@fs.fed.us

C. A. Hatfield
Statistician
USDA Forest Service
Forest Products Laboratory
Madison, WI 53726
E-mail: cahatfield@fs.fed.us

(Received March 2012)

Abstract. Standing stress wave measurements were taken on 274 small-diameter Douglas-fir trees in western Montana. Stand, site, and soil measurements collected in the field and remotely through geographical information system (GIS) data layers were used to model dynamic modulus of elasticity (DMOE) in those trees. The best fit linear model developed resulted in an adjusted $R^2 = 0.52$ for predictions of individual tree DMOE and an $R^2 = 0.85$ for predictions averaged on a stand basis. The linear model used was mean annual increment^{-1}, total tree height, and a GIS-based estimate of soil bulk density. Logical models were also developed to predict membership in dichotomous DMOE categories with 71-82% selected trees meeting their respective DMOE criteria. The inverse relationship between soil bulk density and DMOE could be explained by the soil–tree moisture interactions know as least limiting water range.

Keywords: Douglas-fir, nondestructive, MOE, prediction, soil, stand, least limiting water range (LLWR).

INTRODUCTION

Small-diameter Douglas-fir (*Pseudotsuga menziesii* var. *glauca*) trees are often available from thinning operations in overstocked stands in the Interior Northwest. Douglas-fir can occupy a greater variety of habitats than any other western tree species, from low-elevation grasslands to the lower reaches of the timberline across varied habitat types and disturbance regimes (Burns and Honkala 1990). Corrective management, including commercial thinning, can be used to maintain forest health or return species

* Corresponding author
† SWST member

© 2013 by the Society of Wood Science and Technology

compositions to historic conditions. Thinning operations often produce small-diameter material with small end diameters of less than 20.5 cm. These materials are often manufactured into relatively low-value nonstructural products (posts, pulp, fuel, etc) or low-value structural materials such as studs. Sometimes, these materials are piled and burned.

Prior studies (Green et al 2005) have found that small-diameter coastal Douglas-fir harvested from northern California provided excellent yields of high-quality structural material, characterized by small knots and high stiffness, when sawn to dimensional lumber. Also, use of small-diameter trees as structural roundwood has been proposed as a more efficient use of the resource (Wolfe and Murphy 2005), and recent studies have shown there is potential for using mechanical grading systems to evaluate structural properties of small-diameter logs for engineered applications (Green et al 2008). The potential exists to market these small-diameter materials to manufacturers of high-performance, higher end-value structural uses.

In general, wood stiffness is well correlated with density, and prior research has demonstrated that wood density is one expression of a tree's response to the environment. One of the key elements to understanding variation in wood density, and by extension stiffness, is the relative proportion of latewood to earlywood. Researchers have shown that irrigation or climatic fluctuations can significantly advance or retard the transition from earlywood to latewood and affect the duration of the latewood period (Zahner et al 1964; Brix 1972; Robertson et al 1990). Researchers found that irrigated trees with ample soil moisture made the transition from earlywood to latewood later in the growing season, and adequate soil moisture levels late in the growing season increased the latewood period. Crown structure has also been found to influence latewood period. In a study of the effects of the defoliating disease Swiss needle cast in Pacific Douglas-fir, researchers found increasing latewood proportion associated with shorter crowns in afflicted trees (Johnson et al 2005). Johnson et al (2005) postulated that the loss of needles decreased photosynthetic capacity during the early growing season, which provided the trees with more available resources later in the growing season when latewood was being produced.

Using a stress wave speed measurement on standing trees, in conjunction with tree density measurements, has been shown to provide reasonable estimates of modulus of elasticity (MOE) and, therefore, the structural utility of wood from those trees. Literature reported by practitioners of this method suggests that these stress wave measurements can account not only for the variation in clear wood MOE among trees, but also knots or other grain distortions (Chauhan and Walker 2006; Grabianowski et al 2006; Wang et al 2007). Field measurements of stress wave speed and density are time-consuming, however, which suggests that other indicators that can predict structural quality or focus sampling efforts are needed.

Models to predict MOE in standing trees from stand variables and tree measurements have been proposed for several species. Average values for MOE of lumber cut from Black spruce (*Picea mariana*) in eastern Canada were modeled in plantation and even-aged naturally regenerated stands (Lei et al 2005; Liu et al 2007). The models developed had similar goodness-of-fit measures with R^2 values of 0.55 and 0.56, respectively. MOE predictions in plantation-grown radiata pine (*Pinus radiata*) were effectively modeled ($R^2 = 0.96$) using a combination of stand and soil variables across forested sites in New Zealand (Watt et al 2008).

The primary objective of this study was to develop a model using standard forest inventory data in combination with remotely sensed data to decrease the need for acoustic testing in mixed age stands of suppressed small-diameter Douglas-fir. The models were developed to provide tree-level predictions of dynamic modulus of elasticity (DMOE). Forest managers could use predicted results derived from existing inventory data in combination with additional nondestructive testing to delineate stand boundaries that would deliver a sale with an appropriate average

and variation in DMOE to producers of high-performance structural lumber and composite products. The model would help focus nondestructive testing efforts on the highest quality stands and decrease the number of measurements taken in stands with lower likelihood of producing high-quality lumber products.

MATERIALS AND METHODS

This study focused on small-diameter (<30.5 cm diameter at breast height [DBH]) Douglas-fir stands in the Trapper Bunkhouse management area within the Darby Ranger District of the Bitterroot National Forest in western Montana (Ravalli County, MT). The Trapper Bunkhouse region is a complex landscape of roughly 9300 ha located between the Selway-Bitterroot Wilderness area to the west and state and private property adjacent to the Bitterroot River to the east.

The study area was chosen because of its geography, history, biology, and current management plans. The area has good road access to stands from the Bitterroot River valley to the Wilderness boundary and elevations ranging from 1.190-2.100 km. Past logging practices focused on removal of high-grade ponderosa pine. This, in addition to the exclusion of fire, has led to dense stands of small-diameter Douglas-fir. Typical of overstocked stands in the inland Northwest, forest health concerns included high rates of infection from dwarf mistletoe, a variety of tree diseases, and several species of boring insects. Stumpage for low value uses (pulp, poles, etc) was considered too low to profitably remove harvested material from the study area.

Field Measurements

The preliminary sampling strategy for this study was to measure small-diameter Douglas-fir at four different elevation zones and four crown closure categories (Table 1). Areas meeting the crown closure and elevation criteria were targeted for field data collection. All sites sampled were located on generally north- to east-facing aspects favorable to growth and were naturally regenerated.

Table 1. Preliminary sampling matrix for small-diameter Douglas-fir.

	Number of small-diameter trees to be sampled			
	Percentage crown closure on plot			
Elevation (m)	10-25%	25-40%	40-60%	60-100%
1280-1490	24	24	24	24
1490-1700	24	24	24	24
1700-1910	24	24	24	24
1910-2120	24	24	24	24

Plot centers were located such that discontinuities such as roads, large openings, or other nonforested areas were not part of the plot and stand conditions were consistent. Plots within the same stand were spaced at least 60 m apart. Inventory data collected at each plot included:

- A variable radius plot capturing between three and seven trees per plot for the basal area measurement;
- Crown closure measured with a spherical densitometer to verify percentage canopy closure from a geographical information system (GIS);
- Latitude/longitude of plot center with a global positioning system (GPS);
- DBH and total tree height (TTH) of all trees in the plot (broken top heights were estimated); and
- Slope (%) and aspect (degrees) at plot center.

In addition, three Douglas-fir trees were selected at each plot to provide additional data. Of the trees between 10.2- and 30.5-cm DBH on each plot, the largest, the smallest, and one closest to 20.3 cm had the following measurements and samples taken:

- A stress wave speed measurement, determined using a Fiber-Gen (Christchurch, New Zealand) Director ST-300, was taken from the uphill side above any gross defect such as scars, sweep, or mistletoe/growth defects.
- A clear 12.5-mm increment core was extracted at breast height from the same uphill face and diameter and length measurements of the cores.
- Percentage live crown was recorded.

- Length of branch-free bole (clear bole height) was recorded.

Stress wave and core measurements were used to estimate DMOE of trees.

Analysis

Specific gravity on a green volume basis and tree age were determined from each increment core. Tree age was divided by DBH to calculate the inverse of mean annual increment (MAI^{-1}) for the trees.

An estimation of standing tree DMOE was made by combining the squared stress wave speed with an estimated green bulk density based on the increment core-specific gravity. Wood bulk densities were calculated using an assumed MC of 35%:

$$\mathrm{DMOE} = \frac{\rho}{g} V^2 \qquad (1)$$

where $\rho = 1000\left(\frac{\mathrm{kg}}{\mathrm{m}^3}\right) \times (\text{green specific gravity}) \times (1.35)$; $g = 9.806\left(\frac{\mathrm{m}}{\mathrm{s}^2}\right)$, V = stress wave velocity $\left(\frac{\mathrm{m}}{\mathrm{s}}\right)$

Remotely Sensed Data

GPS locations of the plot centers were overlaid on several GIS data layers. Mapping was performed using ArcGIS 9.1 (ESRI Inc., Redlands, CA). The GIS data layers comprised:

- Potential vegetation type (PVT) classification of western Montana and central Idaho (USDA 2004a): dominant vegetation, tree size, and percentage crown closure for each plot was extracted and assigned categorical values.
- SSURGO soil map 647 (USGS-NRCS 2006): soil properties from the USGS-NRCS soil survey were extracted for each plot location. The soil properties were converted to a weighted average of soil properties encountered in soil layers above obstruction. The resulting indices were organic matter index (% organic matter by weight), pH index (pH), sand index (% sand by weight), silt index (% silt by weight), clay index (% clay by weight), cation exchange capacity index (mEq per 100 g), bulk density (BD) index (kilogram per cubic meter at 0.33 bar moisture tension), and maximum observed root depth (cm). These indices represent the soil properties one would expect if the NRCS standard O, E, A, B, and C soil layers were excavated and thoroughly mixed.
- Preliminary geologic map of the Nez Perce Pass quadrangle (Berg and Lonn 1996): used to assign underlying parent materials for each of the plots.
- Wetness differential (USDA 2004b): wetness index represented the relative drying for each mapping unit from Landsat measures of soil wetness.

Statistical Data

Correlation between stand characteristics and estimated tree MOE was assessed using SAS (SAS Institute, Inc., Cary, NC). Theoretical and logical models were developed to predict DMOE of trees sampled during the field research. Our approach was to divide data into two subsets, one for model calibration and one to test the model. The calibration data set was built from one randomly selected tree from each plot. The remaining trees formed the data set used to test the model. Thus, data from 83 trees were used to build the models, and data from 164 trees were used to test the fit of the models. Initially, all variables were regressed individually with DMOE. Variables with potential for predictive ability were assessed to see if transformations or rearrangements to the variables would improve predictive ability. Using multiple data sets allowed for more aggressive transformations of the variables in the model-building phase. Transformations that performed well using the calibration subset were applied to the test subset during the model testing phase, essentially testing the models with a new data set. This approach was used to decrease the opportunity for overfitting the models.

The theoretical models were developed by stepwise regression on the calibration data set. The

models shown in the results of this study represent a few of the best performing models from the analysis based on their goodness of fit.

The development of logical models stemmed from a stepwise discriminant function analysis performed using SAS and visual analysis to determine which variables best grouped the trees in dichotomous categories (ie greater than or less than 10.3 GPa and greater than or less than 12.4 GPa) and the cutoff values for those variables. The models were built using the smaller calibration data set, and once the models were finalized, they were tested using the larger test data set.

RESULTS

During the fieldwork, it became apparent that the lowest percentage crown coverage conditions indicated by the PVT classification information were not present within the study area. The spatial resolution for PVT was 90 × 90 m, and the lowest crown closures on north or east aspects were actually very dense clumps of trees surrounded by rock or other nonforested areas, especially at high elevations. Because these low crown closure stands did not contain open grown trees as expected in a stand with low levels of crown closure, it was decided to combine the two lowest crown closure classes. Table 2 shows the actual sampling distribution for small-diameter Douglas-fir trees.

Table 3 provides a synopsis of the characteristics of the small-diameter Douglas-fir sampled during the fieldwork. The average tree age of 75 yr and average height of 14.2 m suggests that many of the trees sampled during this study were severely suppressed. The range of specific gravities (0.346-0.530) matched records from the 1965 western wood density survey (FPL 1965) for Ravalli County (0.35-0.53), and the average specific gravity for all trees was likewise consistent with that report.

Table 2. Distribution of small-diameter Douglas-fir trees sampled by elevation and percentage crown closure.

	Number of small trees sampled		
	Percentage crown closure on plot		
Elevation (m)	10-40%	40-60%	60-100%
1280-1490	6	33	27
1490-1700	21	26	33
1700-1910	18	18	23
1910-2120	0	18	24

Table 3. Average tree and stand variables for the 247 small-diameter Douglas-fir trees sampled.

Tree variable[a]	Average[b]
Percentage crown closure (%)	57 (33%)
Basal area on plot (m^2)	10.8 (48%)
DBH (cm)	22.1 (25%)
Total tree height (m)	14.2 (27%)
Percentage live crown (%)	63 (35%)
Mean annual increment^{-1} (yr/cm DBH)	3.5 (39%)
Stress wave speed (m/s)	4152 (13%)
Specific gravity	0.45 (7%)
Age at breast height (yr)	75 (39%)
DMOE (GPa)	10.7 (29%)

[a] DBH, diameter at breast height; DMOE, dynamic modulus of elasticity.
[b] Numbers in parentheses are coefficient of variation.

At this stage of our analysis, we obtained and added NRCS soil typing information for each plot. Because the soil typing information was added after field sampling, there was no systematic sampling across soil types or soil characteristics in this study. A total of 18 different soil types was found to exist within our study area.

Theoretical Models

Table 4 shows the most promising theoretical models built using the smaller calibration data subset. The theoretical model with the best fit was made by combining MAI^{-1}, low BD index (where BD index > 1.46 mg/m^3 = 0, BD index < 1.46 mg/m^3 = 1), and TTH. This model was able to account for 55% of the variation in the samples. The elevation and percentage crown closure variables on which the study was designed were of limited use in predicting DMOE.

To test the model's fit with a new data set, DMOE was regressed against MAI^{-1}, TTH, and low BD index with the larger test data subset (Table 5). Although the goodness of fit dropped from the calibration to the test data subset, it still was able to account for about half the variance

Table 4. Selected theoretical models developed.[a]

Variable types	Variables					Adjusted R^2
Remotely sensed variables	Recoded coverage class[b]	Wetness index[c]	Categorical BD	pH index[c]	Sand index[c]	0.48
	Low BD index[c]	Wetness index[c]	Elevation	Silt index[c]		0.45
Stand-based variables	Percent foliage	Foliage length	DBH	Clear bole ht		0.39
	Percent Foliage	Foliage length	DBH			0.36
Inventory variables	Age maximum 130[d]	MAI^{-1}				0.45
Combined variables	Low BD index	MAI^{-1}	TTH			0.55

[a] BD, bulk density; DBH, diameter at breast height; MAI, mean annual increment; TTH, total tree height.
[b] Recoded coverage class: remotely measured coverage class values were linearized to reflect increase in dynamic modulus of elasticity across classes.
[c] Index values: see Remotely Sensed Data section.
[d] Age maximum 130: age for all trees was capped at 130 yr; trees older than 130 yr were past the value of 130 yr.

present in the test data subset. MAI^{-1} accounted for the most variance followed by TTH and low BD index. The coefficients did not change significantly from the calibration to the test data set ($|t| < 1$). Because regression results from the calibration and test data set were similar, the final proposed model was built using both subsets of data (Table 6).

The final model is therefore

$$\text{Dynamic MOE} = 3.02 + 1.06 * \text{MAI}^{-1} + 0.242 * \text{TTH} + 2.09 * \text{low BD index}$$

With an adjusted R^2 value of 0.52, the model accounts for just more than half of the variance in the combined sample sets. From the standardized coefficient values in Table 6, MAI^{-1} was the most influential variable followed by TTH and low BD index. The root mean squared error (RMSE) for the final model was 2.13 GPa.

Figure 1a shows the fit of the final model developed using both data sets with DMOE measured for those trees. The thicker 95% confidence lines represent the predicted value $\pm$ RMSE $\times$ 1.96. Figure 1b shows the residual plot of the regression of predicted DMOE on measured DMOE. An analysis of the standardized residuals from the regression of measured on predicted values of DMOE indicated a random normal distribution of the residuals across the range of predicted values.

The intent of this model was to help forest managers identify stands with the potential for growing high stiffness material. To that end, Fig 2a

Table 5. Regression results from mean annual increment $(MAI)^{-1}$, bulk density (BD) group, and total tree height (TTH) using larger test subset of data.[a]

	R^2	Adjusted R^2	Root MSE	Mean DMOE (GPa)	
	0.493	0.483	2.19	10.6	
Model	Sum of squares	df	Mean square	F value	Pr > F
Regression	747.2	3	249.1	51.80	<0.0001
Residual	769.1	160	4.807		
Total	1516	163			
Source	Unstandardized coefficients	Standard error	Standardized coefficients	t	Pr > F
Intercept	2.65	0.812		3.27	0.001
MAI^{-1}	1.07	0.134	0.460	7.99	<0.0001
TTH	0.257	0.047	0.320	5.53	<0.0001
Low BD index	1.94	0.423	0.272	4.60	<0.0001

[a] MSE, mean square error; DMOE, dynamic modulus of elasticity; df, degrees of freedom.

Table 6. Final proposed model using both data sets.[a]

F value regression	R^2	Adjusted R^2	RMSE	Mean DMOE (GPa)	
85.92	0.515	0.509	2.13	10.7	
Parameter	Unstandardized coefficients	Standard error	Standardized coefficients	t	Pr > F
Intercept	3.02	0.629		4.80	<0.0001
MAI^{-1}	1.06	0.105	0.465	10.1	<0.0001
TTH	0.242	0.036	0.304	6.63	<0.0001
Low BD index	2.09	0.333	0.295	6.26	<0.0001

[a] RMSE, root mean square error; DMOE, dynamic modulus of elasticity; MAI, mean annual increment; TTH, total tree height; BD, bulk density.

shows the fit of average predicted DMOE and average measured DMOE at the stand level and Fig 2b shows the fit of the standard deviation in DMOE measured in the stands regressed against the standard deviation in DMOE predicted in those same stands. The extreme stand in Fig 2b was a collapsing mixed age stand in which 200-yr-old trees grew alongside 30-yr-old trees.

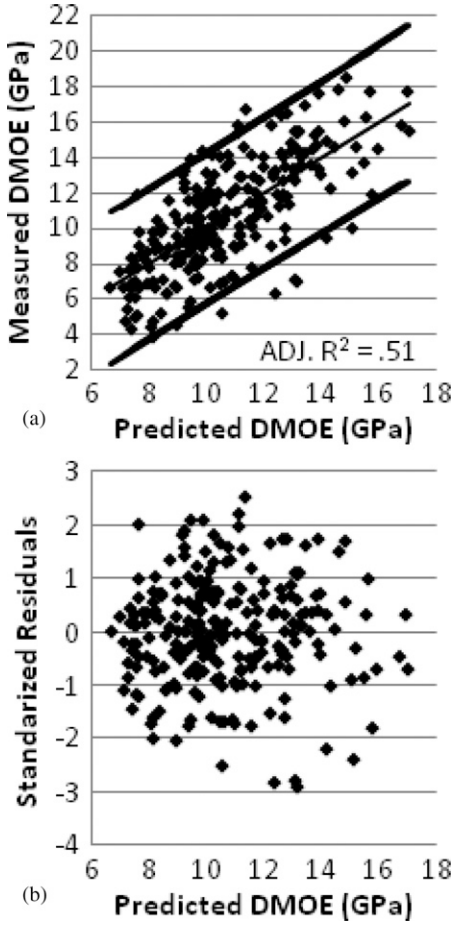

Figure 1. (a) Model fit for both data sets with 95% confidence intervals; (b) standardized residuals from regression of predicted dynamic modulus of elasticity (DMOE) on measured DMOE.

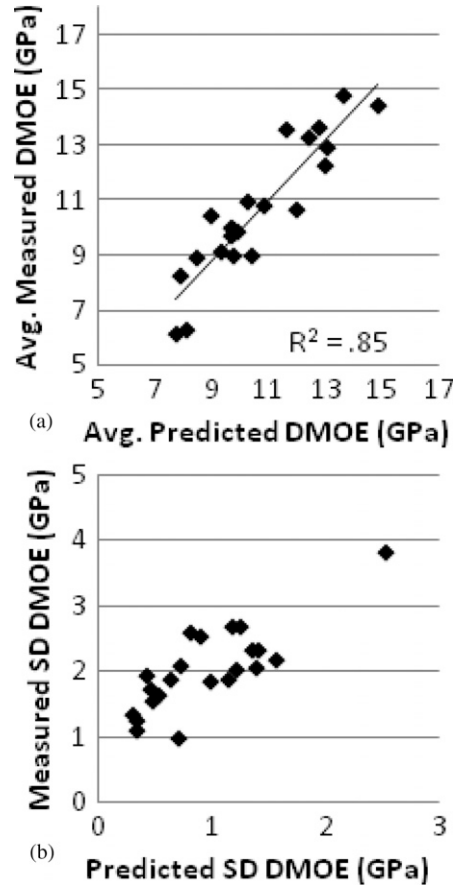

Figure 2. (a) Average measured dynamic modulus of elasticity (DMOE) and average predicted DMOE by stand; (b) standard deviation (SD) of measured DMOE and SD of predicted DMOE at the stand level.

MAI^{-1} was the most significant predictor of DMOE. Figure 3 shows a comparison of the average measured DMOE by MAI^{-1} quartile with one standard deviation error bar for each group and letters representing Scheffe's comparison of means. The Scheffe's comparison of means for the quartiles shown in Fig 3a showed that the lowest, middle two, and highest quartiles had significantly different average measured DMOE with $p < 0.05$ for all comparisons among the three groups. MAI^{-1} was positively correlated with the DMOE value measured for the trees. As shown in Fig 3b, there is an increasing trend in DMOE with increasing MAI^{-1} but little difference in measured DMOE in trees with MAI^{-1} values greater than 6 yr/cm DBH.

TTH was shown to be a significant predictor of DMOE in these stands. Tree age would more likely be chosen in the model building process, but TTH was virtually uncorrelated with MAI^{-1} ($r = 0.083$) with a moderate correlation to DMOE ($r = 0.398$), whereas tree age was highly correlated with MAI^{-1} ($r = 0.7$). From a statistical perspective, independence of TTH from MAI^{-1} made it a more useful predictor than tree age, and it may act as a surrogate for tree age.

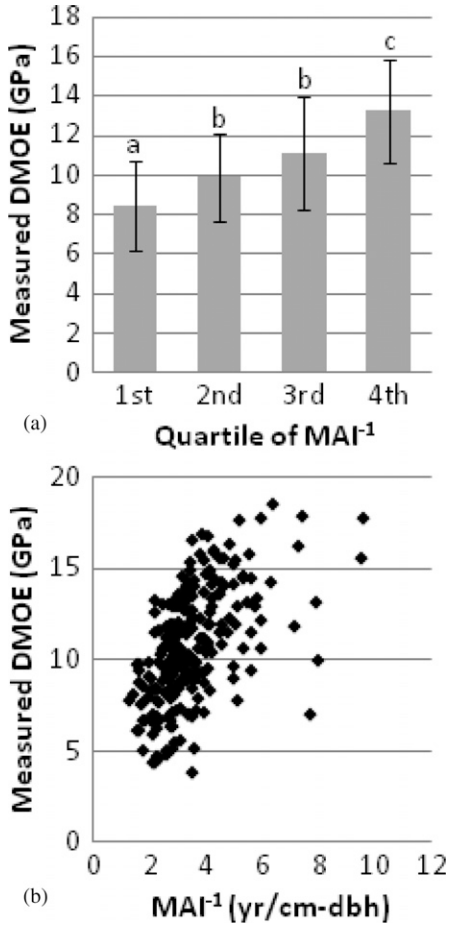

Figure 3. (a) Average dynamic modulus of elasticity (DMOE) by mean annual increment $(MAI)^{-1}$ quartile (error bars represent one standard deviation); (b) MAI^{-1} and DMOE (DBH, diameter at breast height).

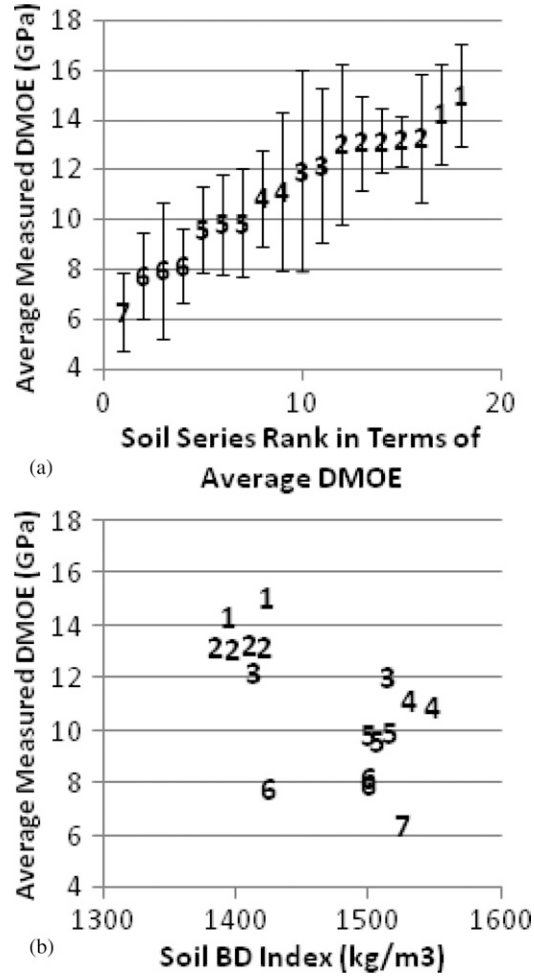

Figure 4. (a) Results of clustering for average dynamic modulus of elasticity (DMOE) for the soils (error bars represent one standard deviation); (b) comparison of average DMOE and bulk density (BD) index for each soil.

The analysis suggested that soil bulk density was negatively correlated with measured DMOE for the trees sampled. Figure 4a shows the clustering of average DMOE measured in the trees from each soil type, and Fig 4b shows average DMOE from each soil type plotted against that soil's BD index. Clustering in Fig 4a was done visually using obvious gaps in average measured DMOE to delineate groups. In Fig 4b, trees on soils with lower BD index had higher average DMOE values with the exception of one soil in Group 6. These aggregations led to the use of the categorical low BD index variable in the theoretical models mentioned previously and provided an important starting point for the logical models described in the following section. Although not shown here, models using the BD index as a continuous variable performed virtually identical to those using BD as a categorical variable.

Logical Models

Logical models were also built to predict memberships into dichotomous DMOE categories. Again, the models were built with the smaller calibration sample set and then tested with the larger test subset. Results from the test subset are reported here. The following methods were developed to identify trees with DMOE greater than 10.3 GPa, greater than 12.4 GPa, and less than 7.6 GPa. In all three logical models, soil BD was the most important factor for selection.

The three columns on the right side of Table 7 contain the results when the logical models were applied to the test subset. The results columns summarize the percentage of trees in the test subset selected by the model that actually met the DMOE criteria of the model, the percentage of the targeted trees the models selected from the test subset, and the percentage of the test subset that met the DMOE criteria. For example, Rule 1 of the model to select trees with DMOEs greater than 10.3 GPa selects all trees on soils with BD index less than 1.46 mg/m^3. For those trees selected by the model, 82% actually had measured DMOEs greater than 10.3 GPa, 39% of all trees in the test subset with DMOEs greater than 10.3 GPa were selected, and trees with DMOEs greater than 10.3 GPa represented 51% of test subset.

DISCUSSION

The models presented were able to make reasonable predictions of DMOE at both the individual tree and stand levels. The 95% confidence interval for predicting individual trees would encompass a range of approximately $\pm$ 4.2 GPa and is admittedly large, but these predictions were made on multiple-aged stands with widely varying stocking levels, site histories, and environmental conditions along an 800-m elevation gradient. Trees with extreme values of age or MAI^{-1} that may have been potential outliers were retained to improve overall robustness of the model at the expense of goodness of fit.

Table 7. Rules for selection of trees meeting given criteria.[a]

Model criteria	Rule no.	Rule	Trees selected by model meeting DMOE criteria (%)	Targeted trees selected by model (%)	Test subset meeting DMOE criteria (%)
Select trees with DMOE > 10.3 GPa	1	BD index < 1.46 mg/m^3	82	39	51
	2	Add trees with BD index > 1.46 mg/m^3 and elevation > 1800 m	72	73	51
Select trees with DMOE > 12.4 GPa	1	BD index < 1.46 mg/m^3 and remotely measured % crown closure = high	73	77	29
Select trees with DMOE < 7.6 GPa	1	BD index > 1.46 mg/m^3 and sites with soil pH < 5 or sites with soil pH > 6 and trees with % crown closure < 30%	71	34	18

[a] DMOE, dynamic modulus of elasticity; BD, bulk density.

Models developed by this research were able to identify stands with high and low average DMOE. The stand level results of the theoretical model shown in Fig 2a suggest that at the stand level, there was a strong correlation between average measured and average predicted DMOE. A common criticism of presenting stand level results is the masking of variance in the measure of interest within the stands, but because the theoretical model was built on an individual tree basis, Fig 2b suggests that the model can provide a forest manager with expected variation in DMOE within a stand, resulting in a more informed decision as to which stands to further investigate for marketing to manufacturers of high-performance lumber and composite materials.

Results of the logical models in Table 7 suggest that using the BD index in conjunction with another remotely measured variable was a powerful selection tool to identify stands with a high proportion of trees with high DMOE or a high proportion of trees with low DMOE. For example, the model was able to identify stands in which more than 70% of the trees sampled had DMOE greater than 12.4 GPa. Variables used in the logical models were all remotely collected and are currently publically available, which implies that a forest manager could perform a great deal of screening from the office in remote areas for which no inventory data are available. As with the theoretical model, the logical models are meant to direct the deployment of nondestructive testing efforts to those stands with the highest probability of producing high stiffness lumber.

Based on standardized coefficients and t scores from the regression results shown in Table 6, MAI^{-1} was the most significant predictor of DMOE. Slow growth has been associated with higher wood density (Johnson et al 2005), especially when coupled with elevated latewood percentages in the annual rings. Slow growth combined with increasing latewood proportions could likewise be associated with higher stress wave speed because of increased proportion of high stiffness latewood. DBH was negatively correlated with stiffness in even-aged black spruce stands (Lei et al 2005; Liu et al 2007), indicating that slow growth was also associated with higher stiffness in those studies. Slow growth associated with high levels of competition for light between trees may also be correlated to fewer and smaller diameter branches, which could result in higher stress wave speed.

TTH was another logical choice for the theoretical models of DMOE because it may have acted as a surrogate for tree age. The average age of trees sampled during this research was 75 yr, but there were 20 trees less than 30 yr old. We would expect the influence of juvenile wood and high microfibril angle to be greatest in those younger trees and decreasing influence in older trees but not linearly into perpetuity. Trees sampled showed a trend of increasing DMOE with tree age up to approximately 130 yr at which point there was no further increase in DMOE. TTH may function as a substitute for a capped age variable for these suppressed trees.

Although soil BD may be influential in many tree–soil interactions, its role in plant-available moisture appeared to be the most likely avenue of influence for stiffness. The concept of least limiting water range (LLWR) (Letey 1985; Da Silva et al 1994; Schoenholtz et al 2000) suggests that for a given soil BD, there will be a range of soil moisture contents between which a plant can extract water from the soil. The upper limit of the range is either the moisture content at which roots are deprived of oxygen or the field capacity in a saturated soil, and the lower limit of the range is the moisture content at which the soil is too hard for roots to penetrate or the wilting point. Increasing soil BD is associated with a narrowing of the limits. Da Silva gives examples of sandy loam soils that exhibit drastic decreases in amount of available water with a 20% increase in bulk density. Figure 5 portrays a slightly exaggerated illustration of the LLWR concept. In very low BD soils, field capacity and wilting point were limiting. As BD increased, lack of oxygen caused by filled pore space (upper limit) and the moisture content at which root penetration was limited (lower limit) were limiting. The latewood initiation moisture

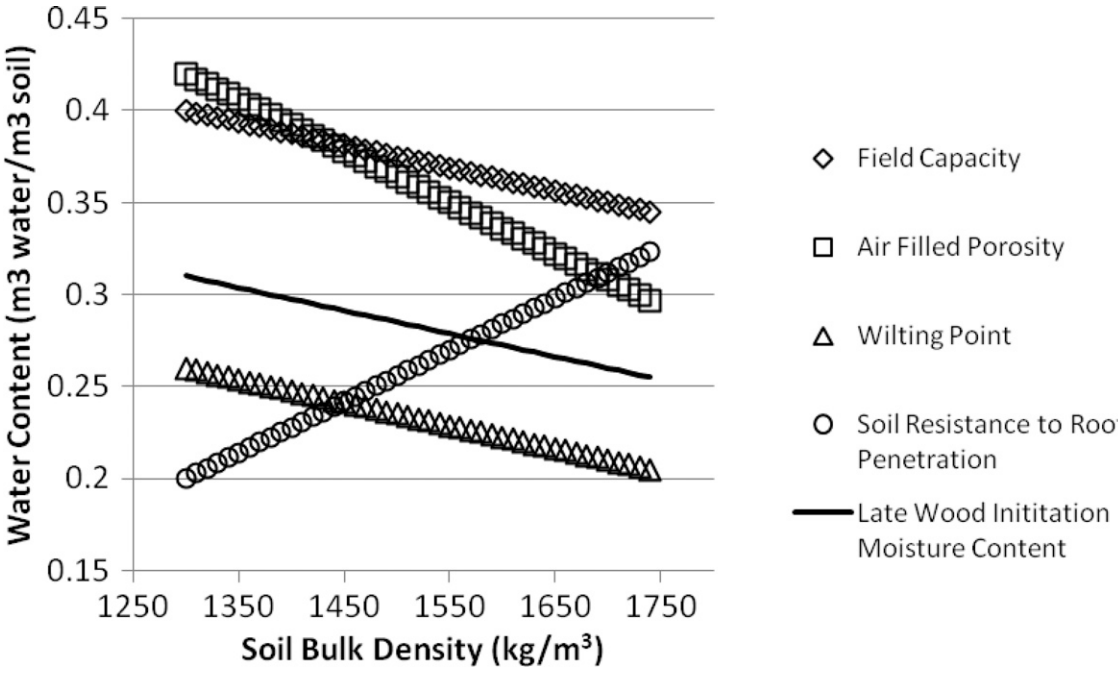

Figure 5. Illustration of least limiting water range concept.

content was drawn to illustrate the potential differences in available moisture content during the latewood period and may not accurately reflect the actual value of the latewood initiation moisture content.

Within the framework of LLWR, BD could influence specific gravity of a given tree both directly within the tree and indirectly through intertree competition. Irrigation and drought have been shown to influence the date of initiation and duration of the latewood production period (Zahner et al 1964; Brix 1972; Josza and Brix 1989). A tree in lower BD soil may have an extended window of available water after the onset of latewood production, leading to higher latewood proportions in the annual rings and higher specific gravity. From a stand-level perspective, if low BD sites have more water available, they might be able to support higher stocking levels with prolonged stem exclusion phases. The increased competition for sunlight could lead to shorter crowns with limited needle retention. Other researchers have found increasing latewood percentages and density with decreasing needle retention in Douglas-fir afflicted with the defoliating disease Swiss needle cast (Johnson et al 2005).

Within the framework of LLWR, soil BD could influence stress wave speed. Within individual trees, higher proportions of high stiffness latewood produced on low BD sites could lead to elevated stress wave speeds. As with specific gravity, if lower BD sites permitted higher stocking, fewer and smaller knots would be produced in the lower bole of the tree. We expect trees with fewer knots to register higher stress wave speeds.

Using the BD index as a variable probably has limitations in its utility to model DMOE. BD index represented a very coarse estimate of average BDs found at a given location and was not spot-checked in the field for this research. As seen in Fig 4b, trees on two relatively narrow ranges of BD index were sampled. The low BD index group ranged from 1.385-1.430 mg/m^3, whereas the high BD index group ranged from 1.5-1.525 mg/m^3. The BD values are clustered such that there was little difference in regressions

using the categorical or continuous values for BD index. The bimodal distribution of BDs forces the assumption of the linear influence of BD index for the range of 1.385-1.525 mg/m^3. The findings of this study are probably restricted to the region in which the data were collected and the range of stand and soil conditions collected therein. Although prior published studies concerning relationships between soil moisture and stress wave speed were not found in the course of this research, specific gravity has been shown to vary with drought severity at the margins of a species' range (Adams and Kold 2004). Variables such as MAI^{-1} and TTH may prove to be transferable, but soil BD may not be an important variable in areas where soil moisture is more or less limiting. Finally, site history was not incorporated into the sampling procedure except to avoid stands that were clearly planted or had received treatments that might bias measurements of stand density.

Future testing involving destructive sampling is needed to verify the models developed in this study. The measurements on which this study is based were nondestructive time-of-flight (TOF) measurements taken through the lower bole of the trees. Experience has shown that TOF measurements have limitations, but short of destructive testing, they are a reasonable starting point for model-building of this type. Expanding the scope of testing to southern and western aspects as well as other suppressed Douglas-fir stands in the inland Northwest would help improve the models presented here.

CONCLUSIONS

In this study, several theoretical and logical models were developed to predict DMOE of small-diameter suppressed Douglas-fir in the wildland–urban interface west of Darby, MT. The models were built using fairly standard inventory data and existing GIS data layers. The proposed final theoretical model incorporated the inverse of MAI^{-1}, TTH, and a remotely collected soil BD measurement and resulted in an adjusted $R^2 = 0.51$. MAI^{-1} and TTH were positively correlated to DMOE. BD of the soils was inversely related to DMOE of the trees found on them and proved to be an important variable for predicting DMOE in both the theoretical and logical models. The logical models for locating trees with DMOE greater than 10.3 GPa, greater than 12.4 GPa, and less than 7.6 GPa were able to identify stands in which more than 70% of the selected trees met their respective criteria using existing GIS data layers. The soil–water–root interaction defined by the LLWR concept may provide an explanation for the importance of soil BD in this study. Soil BD may not be a universally important predictor of wood quality, but future research should consider tree–soil interactions for broad-scale wood quality models.

ACKNOWLEDGMENTS

We thank the Bitterroot National Forest and the staff at the Darby Ranger Station for permission to conduct research and information concerning the Trapper-Bunkhouse Management Area. We thank Dan Loeffler at the Forest Service Rocky Mountain Research Station in Missoula, MT, for providing access to several of the GIS layers used in the study. This project was funded by the Coalition for Advanced Wood Structures at the USDA Forest Products Laboratory in Madison, WI.

REFERENCES

Adams HD, Kold TE (2004) Drought responses of conifers in ecotone forests of northern Arizona: Tree ring growth and leaf C13. Oecologia 140(2):217-225.

Berg RB, Lonn JD (1996) The preliminary geologic map of the Nez Perce Pass 30′ × 60′ quadrangle, Montana, revised 1999, Montana Bureau of Mines and Geology: Open-File Report 339. http://www.mbmg.mtech.edu/gis/gis-datalinks.asp (19 Dec 2011).

Brix H (1972) Nitrogen fertilization and water effects on photosynthesis and earlywood-latewood production in Douglas-fir. Can J For Res 2(4):467-478.

Burns RM, Honkala BH (1990) Douglas-fir *in* Silvics of North America: 1 Conifers. Vol. 2. Agric Handb 654 USDA For Serv, Washington, DC. 877 pp.

Chauhan S, Walker J (2006) Variations in acoustic velocity and density with age, and their interrelationships in radiata pine. For Ecol Mgmt 229(1-3):388-394.

Da Silva AP, Kay BD, Perfect E (1994) Characterization of the least limiting water range of soils. Soil Sci Soc Am J 58(6):1775-1781.

FPL (1965) Western wood density survey. Res Pap FPL-27. USDA For Serv Forest Prod Lab, Madison, WI. 58 pp.

Grabianowski M, Manley B, Walker J (2006) Acoustic measurements on standing trees, logs and green lumber. Wood Sci Technol 40(3):205-216.

Green DW, Gorman TM, Evans JW, Murphy JF, Hatfield CA (2008) Grading and properties of small-diameter Douglas-fir and ponderosa pine tapered logs. Forest Prod J 58(11):33-41.

Green DW, Lowell EC, Hernandez R (2005) Structural lumber from dense stands of small-diameter Douglas-fir trees. Forest Prod J 55(7/8):42-50.

Johnson G, Grotta A, Gartner B, Downes G (2005) Impact of the foliar pathogen Swiss needle cast on wood quality of Douglas-fir. Can J For Res 35(2):331-339.

Josza LA, Brix H (1989) The effects of fertilization and thinning on wood quality of a 24-year-old Douglas-fir stand. Can J For Res 19(9):1137-1145.

Lei YC, Zhang SY, Jiang Z (2005) Models for predicting lumber bending MOR and MOE based on tree and stand characteristics in black spruce. Wood Sci Technol 39 (1):37-47.

Letey J (1985) Relationship between soil physical properties and crop rotation. Pages 277-294 *in* BA Stewart, ed. Advances in soil science. Springer-Verlag, New York, NY.

Liu C, Zhang SY, Cloutier A, Rycabel T (2007) Modeling lumber bending stiffness and strength in natural black spruce stands using stand and tree characteristics. For Ecol Mgmt 242(2-3):648-655.

Robertson EO, Jozsa LA, Spittlehouse DL (1990) Estimating Douglas-fir wood production from soil and climate data. Can J For Res 20(3):357-364.

Schoenholtz SH, Van Miegroet H, Burger JA (2000) A review of chemical and physical properties as indicators of forest soil quality: Challenges and opportunities. For Ecol Mgmt 138(1-3):335-356.

USDA (2004a) Potential vegetation type (PVT) classification of western Montana and northern Idaho (2004). Vector digital data. USDA Forest Service, Northern Region, Missoula, MT. Region 1 Research Station. By permission from Dan Loeffler.

USDA (2004b) Wetness difference: Region 1 Vegetation mapping project (R1-VMP). Raster digital data. USDA Forest Service, Northern Region, Missoula, MT. Region 1 Research Station. By permission from Dan Loeffler.

USGS-NRCS (2006) Soil survey database for Bitterroot National Forest area, Montana, 2006.Vector digital data. http://soildatamart.nrcs.usda.gov (15 July 2007).

Wang X, Carter P, Ross R, Brashaw B (2007) Acoustic assessment of wood quality of raw forest materials—A path to increased profitability. Forest Prod J 57(5):6-14.

Watt MS, Clinton PW, Coker G, Davis MR, Simcock R, Parfitt RL, Dando J (2008) Modeling the influence of environment and stand characteristics on basic density and modulus of elasticity for young *Pinus radiata* and *Cupressus lusitanica*. For Ecol Mgmt 255(3):1023-1033.

Wolfe R, Murphy J (2005) Strength of small-diameter round and tapered bending members. Forest Prod J 55(3):50-55.

Zahner R, Lotan J, Baughman W (1964) Earlywood-latewood features of red pine grown under simulated drought and irrigation. Forest Sci 10(3):361-370.